### Title
Properties of aqueous nitrate and nitrite from x-ray absorption spectroscopy.




### Journal
The Journal of chemical physics, 143(8)

### ISSN
0021-9606



### Authors
Smith, Jacob W
Lam, Royce K
Shih, Orion
et al.



### Publication Date
2015-08-01

### DOI
10.1063/1.4928867

Peer reviewed

# Properties of aqueous nitrate and nitrite from x-ray absorption spectroscopy

Jacob W. Smith, Royce K. Lam, Orion Shih, Anthony M. Rizzuto, David Prendergast, and Richard J. Saykally

Citation: The Journal of Chemical Physics **143**, 084503 (2015); doi: 10.1063/1.4928867
View online: http://dx.doi.org/10.1063/1.4928867
View Table of Contents: http://scitation.aip.org/content/aip/journal/jcp/143/8?ver=pdfcov
Published by the AIP Publishing

# Properties of aqueous nitrate and nitrite from x-ray absorption spectroscopy

Jacob W. Smith,[1,2] Royce K. Lam,[1,2] Orion Shih,[3] Anthony M. Rizzuto,[1]
David Prendergast,[4] and Richard J. Saykally[1,2,a)]
[1]*Department of Chemistry, University of California, Berkeley, California 94720, USA*
[2] *Chemical Sciences Division, Lawrence Berkeley National Laboratory, Berkeley, California 94720, USA*
[3]*National Synchrotron Radiation Research Center, Hsinchu 30076, Taiwan*
[4]*The Molecular Foundry, Lawrence Berkeley National Laboratory, Berkeley, California 94720, USA*

(Received 2 June 2015; accepted 7 August 2015; published online 24 August 2015)

Nitrate and nitrite ions are of considerable interest, both for their widespread use in commercial and research contexts and because of their central role in the global nitrogen cycle. The chemistry of atmospheric aerosols, wherein nitrate is abundant, has been found to depend on the interfacial behavior of ionic species. The interfacial behavior of ions is determined largely by their hydration properties; consequently, the study of the hydration and interfacial behavior of nitrate and nitrite comprises a significant field of study. In this work, we describe the study of aqueous solutions of sodium nitrate and nitrite via X-ray absorption spectroscopy (XAS), interpreted in light of first-principles density functional theory electronic structure calculations. Experimental and calculated spectra of the nitrogen K-edge XA spectra of bulk solutions exhibit a large 3.7 eV shift between the XA spectra of nitrate and nitrite resulting from greater stabilization of the nitrogen 1s energy level in nitrate. A similar shift is not observed in the oxygen K-edge XA spectra of $NO_3^-$ and $NO_2^-$. The hydration properties of nitrate and nitrite are found to be similar, with both anions exhibiting a similar propensity towards ion pairing. © *2015 AIP Publishing LLC.* [http://dx.doi.org/10.1063/1.4928867]

## I. INTRODUCTION

Owing largely to their affordable pricing and excellent water solubility, salts of nitrate and nitrite have found numerous uses in both commercial and laboratory applications. For example, nitrate is an important component of agricultural fertilizers, promoting general and leaf growth, although overuse of such fertilizers has come under significant scrutiny in recent years for its environmental impacts.[1] In addition to their well-known applications in food preservation and similar antimicrobial roles, nitrite anions may prove useful in the complexation of actinides as part of the life cycle of nuclear fuels.[2] In addition, recent studies have indicated that nitrate and nitrite may have therapeutic medical applications in the treatment of numerous conditions, particularly acute cardiovascular events including myocardial infarction and stroke.[3]

Nitrate is of particular importance in environmental chemistry and modeling as a result of its high concentration in atmospheric aerosols.[4] It has become increasingly clear that the chemistry of such aerosols depends substantially on the interfacial behavior of constituent anions.[5,6] Consequently, the behavior of atmospherically abundant ions such as nitrate at the air-water interface has become the subject of substantial study in recent years.[7–11] The results of theoretical investigations of the interfacial behavior of $NO_3^-$ have been inconsistent, with some models predicting interfacial enhancement and others interfacial depletion. Experimental results from ultraviolet second harmonic generation (UV-SHG) spectroscopy indicate a weak surface enhancement,[12] while X-ray photoelectron spectroscopy (XPS)[11] indicates that nitrate is present at the air-water interface at a depleted concentration relative to the bulk. Much of this inconsistency can be attributed to a free energy of adsorption near 0.[12]

Several researchers have proposed that surface affinity is largely driven by the polarizability of the ion in question.[7,8,13] However, while polarizability often correlates with anion surface activity, recent studies have indicated that surface adsorption propensity is more generally controlled by the bulk hydration properties of the anion.[14–16] Both models predict a stronger surface affinity for nitrate than for nitrite. However, UV-SHG investigations of aqueous sodium nitrite have indicated a substantially stronger surface affinity than that observed for the nitrate salts.[17] This surprising result has been attributed to the adsorption of nitrite to the air-water interface as a contact ion pair with the sodium counterion.

In this work, we present the study of aqueous solutions of sodium nitrate and sodium nitrite via X-ray absorption spectroscopy (XAS). XAS provides an atom-specific probe of unoccupied electronic states and is sensitive to both the intra- and intermolecular environment of the target atom. Extraction of meaningful chemical information from XA spectra requires interpretation with the assistance of detailed electronic structure calculations. We have utilized the Prendergast-Galli eXcited electron and Core Hole (XCH) methodology, a first-principles density functional theory (DFT) calculation, to compute theoretical XA spectra of aqueous $NaNO_3$ and

a)Author to whom correspondence should be addressed. Electronic mail: saykally@berkeley.edu.

 

$NaNO_2$ solutions. We have recently used this combination of experimental and theoretical methodologies to study cation-cation pairing in aqueous solutions of guanidinium hydrochloride,[18] the hydrolysis of carbon dioxide in the carbon cycle,[19,20] and the solvation of $Li^+$ by propylene carbonate.[21] Here, we apply these techniques to the comparative study of ion solvation and pairing in aqueous solutions of $NaNO_3$ and $NaNO_2$.

## II. EXPERIMENTAL AND THEORETICAL METHODS

### A. X-ray spectroscopy of liquid microjets

Nitrate and nitrite were used as obtained from EMD Chemical Inc., ACS grade, with 99% minimum purity. Solutions were prepared in 18.2 MΩ cm water obtained from a Millipore system.

XA spectra of the nitrogen K-edge were collected at Beamline 8.0.1 of the Advanced Light Source at Lawrence Berkeley National Laboratory (Berkeley, CA), with nominal resolving power $E/\Delta E = 7000$. Liquid jets of solutions of nitrate and nitrite were generated by pumping the liquid through a 30-$\mu$m inner diameter silica capillary. The liquid jets interact with the focused X-ray beamline (spot size ~100 $\mu$m × 35 $\mu$m) in a vacuum chamber at $\sim 10^{-4}$ Torr. Total electron yield (TEY) XA spectra are collected on a 2.1 kV biased copper electrode with 0.2 eV step sizes and 1 s count time per step. Our previous work has demonstrated that TEY XA spectra are representative of the bulk liquid.[22,23] Spectra have been normalized to $I_0$ signal collected on a high-transmission gold grid intersecting the beamline upstream of the chamber. Spectra of the gas-phase background were measured by moving the jet ~1 mm out of the X-ray beamline and collecting the TEY spectrum; the resulting gas-phase spectra were subsequently subtracted from the corresponding liquid spectra. A single-point energy axis calibration was performed using gaseous nitrogen. A more complete description of the experiment can be found in a prior publication.[24]

### B. Molecular dynamics simulations

Condensed phase molecular dynamics simulations were performed in Amber 14 under periodic boundary conditions.[25] We constructed simulation cells for sodium nitrate and sodium nitrite solvated by TIP3P water molecules[50] in two sizes: small boxes containing ~90 water molecules and larger boxes containing ~550 water molecules. We employed a semi-empircal Quantum Mechanics/Molecular Mechanics (QM/MM) approach utilizing the PM3 semi-empirical quantum-chemical method,[51] while the classical region was simulated using the Amber default ff99SB force field parameters. The quantum mechanical region consisted of the nitrate/nitrite anion and intermolecular interactions of the anion with any cation or water molecule within a defined interaction cutoff distance; this same cutoff distance was utilized for treatment of intermolecular interactions within the classical region of the simulation cell comprising all components aside from the anion. Trajectories of the small boxes were simulated for 20 ns using a 4 Å cutoff for intermolecular interactions, with coordinate snapshots stored every 200 fs. The larger boxes were simulated with 4, 7, and 10 Å interaction cutoffs, with simulation times between 20 and 150 ns and again recording coordinates every 200 fs. More detailed simulation parameters may be found in Tables I and II. Radial distribution functions (RDFs) and integrated RDFs were calculated using the built-in analysis tools of the Visual Molecular Dynamics (VMD) program.[26]

TABLE I. Simulation parameters from MD simulations of sodium nitrate.

| Interaction cutoff (Å) | 4 | 4 | 7 | 10 |
|---|---|---|---|---|
| No. of water molecules | 90 | | 511 | |
| Box dimensions (Å) | 14.584 | | 25.622 | |
| | 13.062 | | 24.324 | |
| | 14.334 | | 25.251 | |
| Concentration (mol/l) | 0.608 | | 0.105 | |
| Run time (ns) | 20 | 82 | 81 | 150 |
| Pairs (%)[a] | 68.2 | 39.8 | 53.4 | 31.2 |

[a]Percentage of snapshots representing an ion-paired configuration.

### C. Simulated spectroscopy

Simulated spectra of the nitrogen and oxygen K-edges of nitrate and nitrite were calculated using the XCH approximation,[27] a first-principles constrained-occupancy DFT electronic structure calculation. Molecular coordinates for the electronic structure calculations were sampled from the small box MD simulation, with snapshots for simulated spectroscopy separated by 160 ps. Fifty snapshots each corresponding to ion-paired ($r_{N-O\ldots Na} \leq 2.6$ Å) and unpaired ($r_{N-O\ldots Na} > 2.6$ Å) configurations were analyzed and averaged for each anion. DFT calculations were performed under periodic boundary conditions using the Plane Wave Self-Consistent Field (PWSCF) program within the Quantum-ESPRESSO package.[28] Exchange correlation potentials were calculated within the Perdew-Burke-Ernzerhof form of the Generalized Gradient Approximation (PBE-GGA).[29] The XCH calculation generates the electron density of the lowest energy core-excited state self-consistently, promoting an electron from a target atom and modeling the impact of the core hole on electronic structure via a suitably modified pseudopotential. Higher energy excited states are approximated from the unoccupied Kohn-Sham orbitals of the self-consistent field generated for the first core-excited state. Transition matrix elements between the 1s atomic orbital of the target

TABLE II. Simulation parameters from MD simulations of sodium nitrite.

| Interaction cutoff (Å) | 4 | 4 | 7 | 10 |
|---|---|---|---|---|
| No. of water molecules | 89 | | 555 | |
| Box dimensions (Å) | 13.080 | | 24.866 | |
| | 14.332 | | 26.542 | |
| | 13.885 | | 25.589 | |
| Concentration (mol/l) | 0.638 | | 0.0983 | |
| Run time (ns) | 20 | 20 | 20 | 20 |
| Pairs (%)[a] | 63.8 | 27.9 | 42.8 | 59.8 |

[a]Percentage of snapshots representing an ion-paired configuration.

atom and calculated unoccupied states are computed within Fermi's golden rule. Resulting transitions were broadened via Gaussian convolution using a fixed linewidth of 0.2 eV to generate the X-ray absorption spectrum of the target atom. The energy scale of the calculated X-ray absorption spectrum of each excited atom, from these plane-wave pseudopotential calculations, is necessarily aligned by reference to a theoretical isolated atom and one experimentally derived constant based on the spectrum of a well-defined system: gaseous $N_2$ and $O_2$ for the N and O K-edges, respectively, as previously described.[19]

## III. RESULTS AND DISCUSSION

XA spectra of the nitrogen K-edge of sodium nitrate and sodium nitrite solutions between 0.5 and 3M are shown in Figure 1. The spectra exhibit two strong features: a sharp feature corresponding to the 1s-$\pi^*$ transition and a broader feature corresponding to the 1s-$\sigma^*$ transition centered ~9.5 eV higher in energy. The spectrum of each anion is found to be invariant with concentration in this range. However, a substantial blue shift of ~3.65 eV (measured at the center of the 1s-$\pi^*$ transition) separates the nitrate spectrum from the nitrite spectrum. This is consistent with similar shifts previously reported between the X-ray photoelectron spectra of aqueous nitrate and nitrite[11] and XA spectra of the solid potassium salts.[30] It is substantially larger than the 1.4 eV shift previously observed in the nitrogen K-edge spectra of aqueous glycine with neutral and protonated (oxidation state +1) nitrogen atoms.[31]

The performed MD simulations do not suggest a statistically significant difference in the ion pairing rates of sodium nitrate and sodium nitrite salt solutions in the small box simulations used for electronic structure calculations. RDFs and integrated RDFs for nitrate and nitrite are shown in Figures 2 and 3, respectively. The local solvent environment is explored based on statistics related to the water oxygen population in the vicinity of the anions (provided from the perspective of their N atoms) and the $Na^+$ cations. Ion-pairing is described in terms of the N-$Na^+$ distribution. Unsurprisingly, increasing the box size from ~90 water molecules to >500 waters substantially decreased the ion pairing probability for both nitrate (from 68% to 22%) and nitrite (from 63% to 28%). It is likely that the ions in the small box used for electronic structure calculations experienced enhanced ion pairing as a result of finite size effects. Also unsurprisingly, increasing the interaction length in the larger box generally increases the probability of ion pairing. There is a decrease in $NO_3^-\ldots Na^+$ ion pairing from the 7 Å cutoff simulation to the 10 Å cutoff simulation, which was reproducible over several simulation runs. The origin of this anomalous behavior is not clear. It is reasonable to assume that the results of the 10 Å cutoff simulations are most accurate within the simulation parameters utilized. However, this is the only set of simulation parameters for which nitrite exhibits a greater propensity for ion pairing than nitrate, whereas experimentally determined activity coefficients for solutions of sodium nitrate[32] and nitrite[33] indicate a greater propensity towards ion pairing in nitrate solutions throughout the concentration range covered in this work. While this does indicate that the small box simulations used in the electronic structure calculations were reasonably representative of the relative rates of ion pairing indicated by the experimental data, the anomalous ion pairing behavior observed in the 10 Å cutoff simulations of the larger system—ostensibly the most accurate simulations performed—presents an interesting matter for future investigation. Correlation curves—calculated by correlation $(dt) = \langle f(t) \cdot f(t + dt) \rangle$ with $f(t) = 1$ for ion-paired configurations, $f(t) = -1$ for unpaired configurations—are shown in Figure 4, fitted to least-squares exponential decay curves. Fit parameters and correlation lifetimes may be found in Table III. The ion-pairing correlation lifetimes for the small box simulations are found to be 121 and 77 ps for $NO_3^-$ and $NO_2^-$, below the 160 ps interval at which parameters were stored for electronic structure calculations.

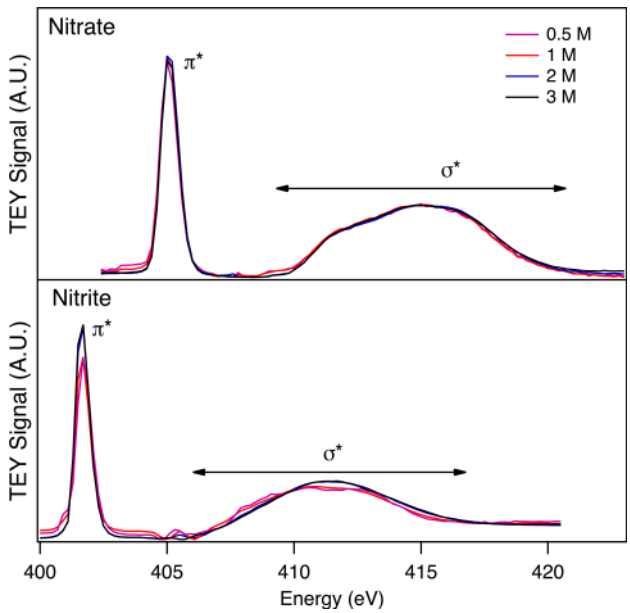


FIG. 1. Nitrogen K-edge TEY XA spectra of solutions of $NaNO_3$ and $NaNO_2$ between 0.5 and 3M. The spectra of each salt are qualitatively similar across the concentration range studied. Annotations indicate the spectral regions corresponding to 1s-$\sigma^*$ and 1s-$\pi^*$ transitions.

The sodium-water RDFs exhibit a maximum for the first solvation shell at 2.4 Å and corresponding minimum between the first two shells at 3.15 Å, consistent with the literature values from experiments and theory.[34–36] The $Na^+$ hydration number obtained by the value of the nRDF at the 3.15 Å minimum is found to be ~4.9. This is slightly lower than previously reported values, but within error of most;[35,37–39] furthermore, the hydration numbers from the small box simulations used for electronic structure calculations are found to be slightly higher at ~5.05.

MD simulations reveal very little difference in the hydration properties of nitrate and nitrite. The hydration of each anion was found to be consistent between the small and large simulation boxes and across interaction lengths, with nitrate and nitrite hydrated by an average of 11.8 and 11.9 water molecules, respectively, in the first shell. These values are somewhat larger than previously reported hydration

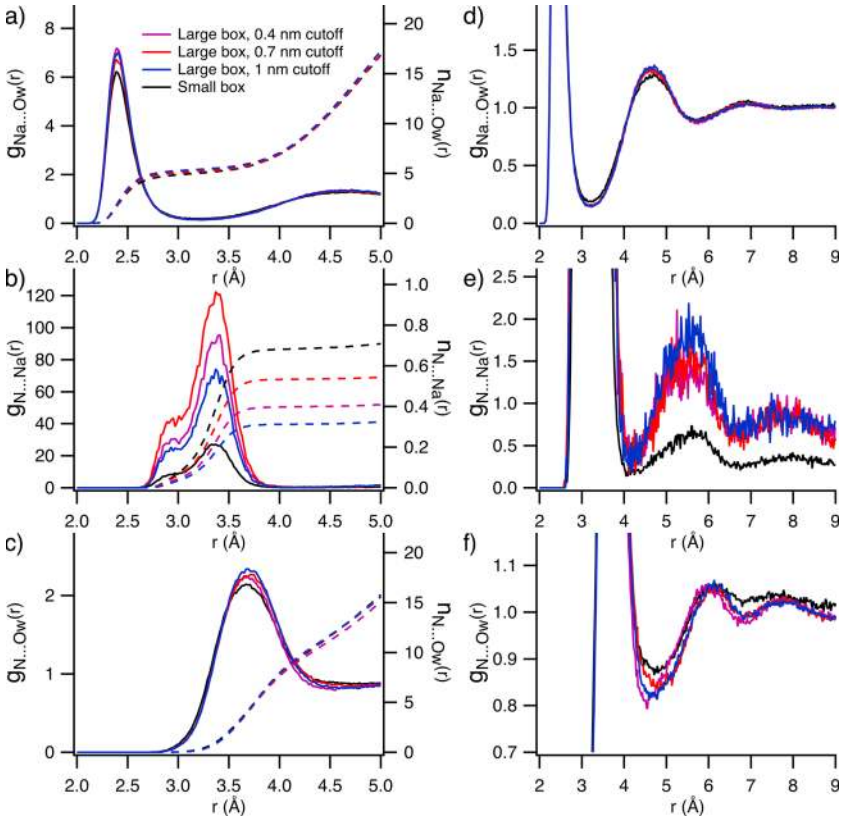


FIG. 2. (a) Radial distribution functions {RDFs, $g(r)$} and integrated radial distribution functions {nRDFs, $n(r)$, shown as dashed lines} for the interaction of the sodium ion with water oxygen in MD simulations of $NaNO_3$; (b) RDFs and nRDFs for the interaction of the sodium ion with nitrate (measured from the position of the nitrogen atom) for the same MD simulations; (c) RDFs and nRDFs for the interaction of the nitrate nitrogen atom with water oxygen; (d)-(f) contain the RDFs from (a)-(c), respectively, extended to longer range and expanded to lower values on the y-axis to show second and third solvation layers in ion-water RDFs and solvent-separated ion pair formation in the ion-ion RDF. The splitting observed in (b) arises from the existence of two distinct ion-pairing configurations, one in which the cation sits between two of the oxygen atoms of the nitrate anion, closer to the nitrogen, and one in which the sodium ion interacts with only one oxygen atom, further from the nitrogen.

numbers from *ab initio* simulations[40,41] and classical MD simulations.[9] Some of this discrepancy is likely explained by differences in the method by which hydration number is calculated. Many previous papers have estimated hydration numbers by the number of hydrogen bond donors or the RDF from the oxygen atoms. We have estimated hydration numbers from the integrated RDF, counting water molecules around the oxygen atoms as well as those directly interacting with the nitrogen center, and effectively including non-bonding or weakly interacting near-neighbors (i.e., not in a

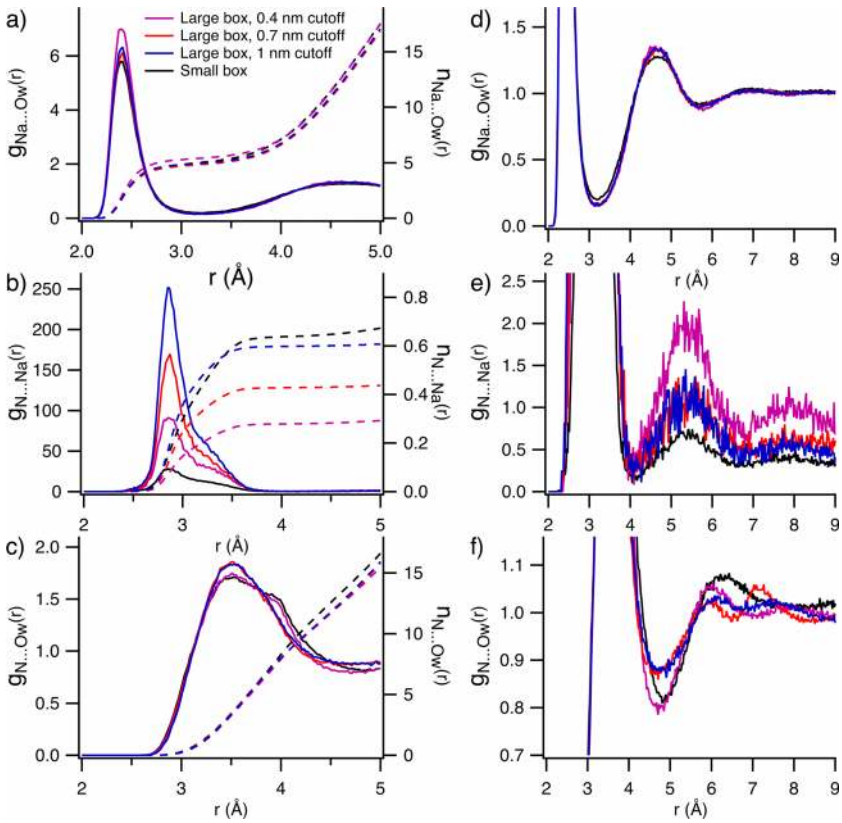


FIG. 3. (a) RDFs $\{g(r)\}$ and nRDFs $\{n(r)$, shown as dashed lines$\}$ for the interaction of the sodium ion with water oxygen in MD simulations of $NaNO_2$; (b) RDFs and nRDFs for the interaction of the sodium ion with nitrite (measured from the position of the nitrogen atom) for the same MD simulations; (c) RDFs and nRDFs for the interaction of the nitrite nitrogen atom with water oxygen; (d)-(f) contain the RDFs from (a)-(c), respectively, extended to longer range and expanded to lower values on the y-axis to show second and third solvation layers in ion-water RDFs and solvent-separated ion pair formation in the ion-ion RDF. The $Na^+ \ldots$ water RDF exhibits different behaviors outside the first solvation shell for different interaction cutoff lengths. This behavior was not observed in the $Na^+ \ldots$ water RDFs for the nitrate simulations, which overlaid well across all interaction cutoffs.

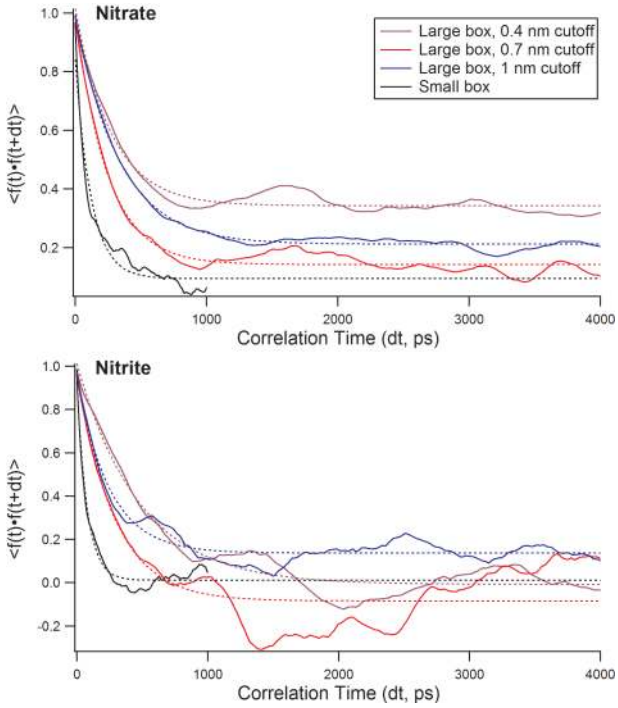


FIG. 4. Correlation functions $\langle f(t) \cdot f(t+dt) \rangle$ for anion-cation interactions in MD simulations of $NaNO_3$ (top) and $NaNO_2$ (bottom). Least-squares best fit exponential decay curves for each correlation function are indicated by dashed lines of corresponding color. Coefficients for best-fit lines and corresponding correlation times are listed in Table I.

traditional hydrogen bond donor geometry with respect to the anion). Experimental estimates of the hydration numbers from scattering and infrared absorption experiments vary substantially,[42–44] with one X-ray diffraction study finding a hydration number for nitrate as high as 17.7.[45] The question of solvation structure is further complicated by the suggestion of Simeon *et al.* that two distinguishable forms of aqueous $NO_3^-$ with differing solvation numbers coexist near room temperature.[46] Furthermore, it has been suggested that the first solvation shell of the nitrate anion, from the standpoint of solvation thermodynamics and polarizability, contains only 3 water molecules,[8,47] suggesting that precise solvation number

TABLE III. Fit coefficients from the least-squares exponential fits of form $f(dt) = Y_0 + Ae^{-dt/\tau}$ to the ion-pairing correlation plots in Figure 4. The first 3 rows for each anion contain the fit parameters to the correlation curves from the large box simulation results with 4, 7, and 10 Å cutoffs for intermolecular interactions, while the fourth line contains the fit parameters for the correlation curve of the small box simulation. The correlation lifetimes τ are found in the last column.

| | Cutoff (Å) | $Y_0$ | A | $1/\tau$ ($ps^{-1}$) × $10^{-3}$ | τ (ps) |
|---|---|---|---|---|---|
| $NO_3^-$ | 4 | 0.342(4) | 0.67(3) | 3.6(5) | 274 |
| | 7 | 0.141(7) | 0.85(6) | 4.1(4) | 242 |
| | 10 | 0.211(2) | 0.782(0) | 3.00(8) | 332 |
| (Small box) | 4 | 0.093(9) | 0.74(7) | 8.2(7) | 121 |
| $NO_2^-$ | 4 | −0.008(3) | 1.02(0) | 2.0(9) | 479 |
| | 7 | −0.08(5) | 1.05(5) | 3.5(1) | 285 |
| | 10 | 0.136(9) | 0.80(9) | 4.0(1) | 249 |
| (Small box) | 4 | 0.011(6) | 0.91(0) | 12.(9) | 77 |

from the integrated RDF may have a limited effect on electronic structure and associated transition dipole oscillator strengths. The maximum of the first peak in the N…$O_{water}$ RDF, corresponding to the first solvation shell, is consistently located at 3.7 Å. This is slightly longer than the average experimental radius of 3.51 Å measured at 25 °C via X-ray diffraction.[48] The maximum of the nitrite N…$O_{water}$ RDF is located closer to the nitrogen, at 3.5 Å; however, this results from the nearer proximity of oxygen to the increased exposure of the nitrogen atom, and the hydrogen bond lengths are similar to those from the nitrate simulations. The first peak of the RDF extends to the same minimum at 4.5 Å as that found for nitrate.

Calculated XA spectra of the nitrogen K-edge for ion-paired and unpaired molecular configurations of $NO_3^-$ and $NO_2^-$ are compared to the experimental spectra in Figure 5. The theoretical spectra accurately reproduce the spectral features observed in the experimental spectra. No significant differences between the ion-paired and unpaired spectra are evident for either anion. This is consistent with the experimental findings of an XAS spectrum independent of solution concentration. A spectral shift of 3.7 eV is observed between the 1s-π* features of nitrate and nitrite, consistent with the 3.65 eV shift between the experimental spectra. The computed valence density of states exhibit no substantial shift in the positions of the available virtual orbitals in the ground state (LUMO shift of ~0.07 eV), indicating that the observed and calculated spectral shift derives from a difference in the energy levels of the nitrogen 1s core levels of nitrate and nitrite. This is consistent with the previously noted similar spectral shift observed in the XPS spectra of the ions.[11]

Isosurfaces of the core-excited LUMO and LUMO+1 states of aqueous nitrate and nitrite are exhibited in Figure 6.

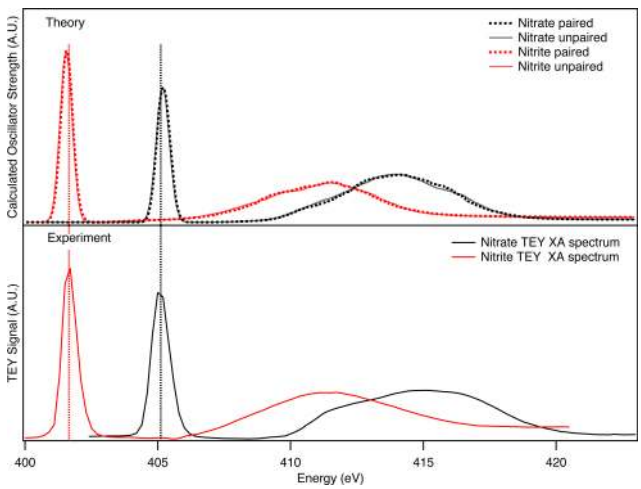


FIG. 5. Calculated nitrogen K-edge XA spectra of ion-paired and unpaired molecular configurations of $NaNO_3$ (black) and $NaNO_2$ (red). The lower panel shows the corresponding experimental spectra for comparison. Experimental and theoretical spectra have both been calibrated via a single-point energy alignment relative to the well-characterized spectrum of $N_2$ gas. The calculated spectra of ion-paired and unpaired molecular configurations indicate that the nitrogen K-edge spectrum is not sensitive to ion pairing. Dashed vertical lines indicate the peak centers of the 1s-π* transition for each anion in the experimental spectrum. The calculated spectrum of $NO_2^-$ matches experiment well; a blue shift of 0.05 eV relative to experiment is observed for $NO_3^-$.

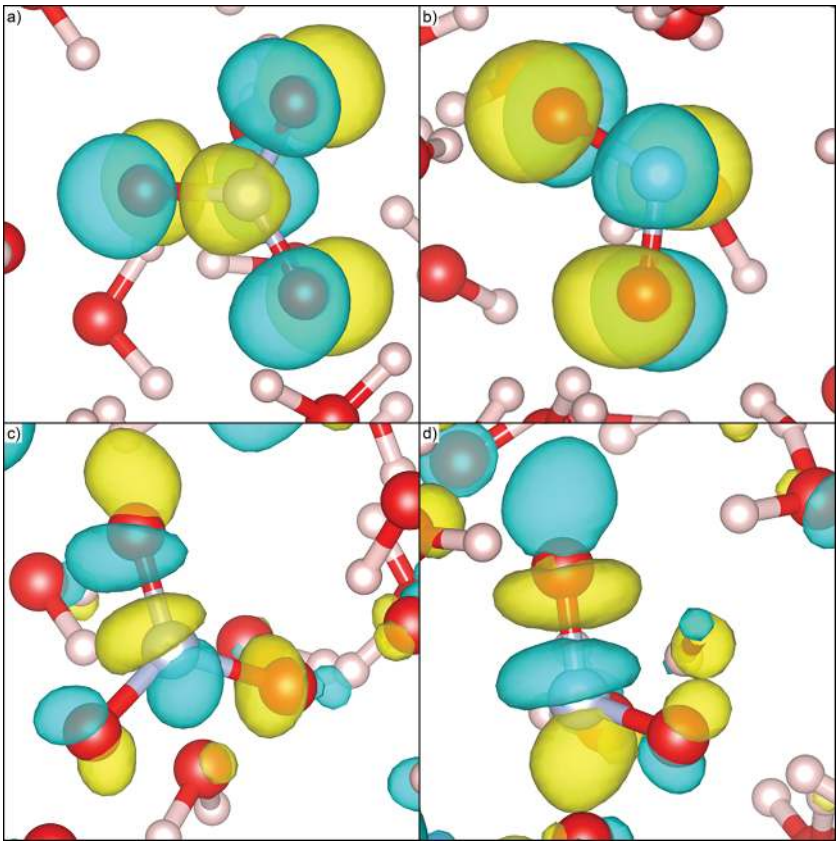


FIG. 6. Isosurfaces of the LUMO and LUMO+1 core excited states of aqueous nitrate and nitrite anions. Images (a) and (b) show the calculated isosurfaces of the LUMO of nitrate and nitrite, respectively. These states exhibit distinctive $\pi^*$ geometry and are almost entirely localized on the anion. Images (c) and (d) exhibit the LUMO+1 of nitrate and nitrite, respectively. These states have primarily $\sigma^*$ character and are highly delocalized; while the displayed image highlights the character of the state on the anion, significant electron density is calculated to exist on water molecules throughout the simulation cell. Some solvent-centered density may be observed here and does not appear to depend on hydrogen bonding or other specific solvent-solute geometries.

The LUMO for each anion exhibits $\pi^*$ symmetry, while the LUMO+1 exhibits primarily $\sigma^*$ character but is highly delocalized, with substantial electron density observed on solvent molecules throughout the simulation cell. The $\pi^*$ LUMO state is highly localized on the ion, with almost no electron density observed on the solvent water. This explains the insensitivity of the spectral feature associated with the transition into this state to the solvation environment of the ion. Similarly, the substantial extent of delocalization observed in the $\sigma^*$ states may explain their calculated and observed spectral insensitivity to the local environment; as the calculated electron density extends well beyond the first solvation shell and does not appear to favor hydrogen-bonded solvent molecules, the state may be sampling the bulk solvent sufficiently to render local structure fluctuations insignificant. Similar electronic structures have previously been found to exhibit spectral insensitivity to the local solvation environment in boron oxides.[49]

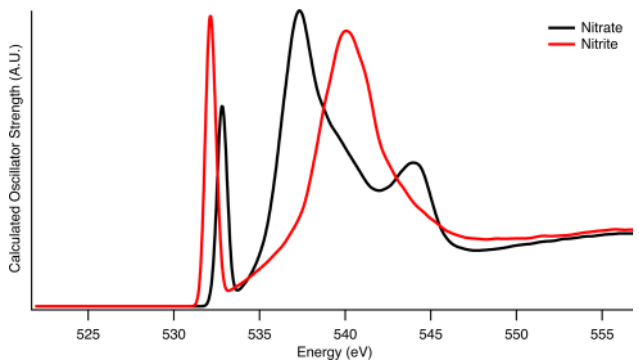


FIG. 7. Calculated oxygen K-edge XA spectra of $NO_3^-$ and $NO_2^-$. Energy calibration was performed relative to the oxygen K-edge absorption spectrum of gaseous $CO_2$. As with the calculated nitrogen K-edge spectra exhibited in Figure 5, the calculated oxygen K-edge spectra of ion-paired and unpaired molecular configurations overlaid nearly exactly. Consequently, only the overall average spectra are displayed here.

We have also computed the oxygen K-edge XA spectra of the nitrate and nitrite anions from the same snapshots; these are displayed in Figure 7. The computed spectra of ion-paired and unpaired snapshots were once again near-identical, and only the average of all snapshots is displayed. Oxygen K-edge spectra are found to be in the same energy range for nitrate and nitrite, indicating the stability in the oxidation state of oxygen atoms (nominally 2-) relative to that of nitrogen which varies depending on the degree of oxidation evident in the nitrate (nominally 5+) and nitrite (nominally 3+) anions. Generally, measurement of the XA spectra of aqueous solutes at the oxygen K-edge is not plausible due to the high-intensity, broad background spectrum of the $H_2O$ solvent. However, the calculated position of the first absorption feature in the O K-edge of aqueous nitrate and nitrite, at 532-533 eV, is slightly lower in energy than the absorption onset of water, and it may be possible to observe this feature in experimental spectra in future studies.

## IV. CONCLUSIONS

We have presented the first XA spectra of aqueous $NO_3^-$ and $NO_2^-$. The hydration properties and ion-pairing propensities of the anions are found to be similar. The XA spectrum

of $NO_2^-$ is red-shifted by 3.7 eV relative to the $NO_3^-$ spectrum; the theory indicates that this shift arises from a relative stabilization of the nitrogen 1s ground state in nitrate. The spectra are found to be insensitive to the local environment; this is likely a result of the localization of the $\pi^*$ state on the anion and delocalization of the $\sigma^*$ state well into the bulk water beyond the first hydration shell. Calculated XA spectra of the oxygen K-edge of nitrate and nitrite do not indicate a substantial shift between the spectra of the two anions.

## ACKNOWLEDGMENTS

The authors thank the staff of the Advanced Light Source for excellent experimental support, with special thanks to Wanli Yang and Jon Spear. Experimental and computational portions of the work described in this paper were supported by the Director, Office of Basic Energy Sciences, Office of Science, U.S. Department of Energy (DOE) under Contract No. DE-AC02-05CH11231, through the Lawrence Berkeley National Lab, Berkeley, California; XA spectra were collected at Beamline 8.0 of the Advanced Light Souce; computational resources for electronic structure calculations were provided by the National Energy Research Scientific Computing Center (NERSC), a DOE Advanced Scientific Computing Research User Facility; and analysis of calculations was performed as part of a User Project at The Molecular Foundry. Computational resources for molecular dynamics simulations were provided by the Molecular Graphics and Computation Facility in the UC Berkeley College of Chemistry under NSF CHE-0840505.

[1]M. A. Sutton, O. Oenema, J. W. Erisman, A. Leip, H. van Grinsven, and W. Winiwarter, Nature **472**, 159 (2011).
[2]F. Dulong, J. Pouessel, P. Thuéry, J.-C. Berthet, M. Ephritikhine, and T. Cantat, Chem. Commun. **49**, 2412 (2013).
[3]J. O. Lundberg, E. Weitzberg, and M. T. Gladwin, Nat. Rev. Drug Discovery **7**, 156 (2008).
[4]R. P. Wayne, *Chemistry of Atmospheres* (Oxford University Press, Oxford, 2000).
[5]S. W. Hunt, M. Roeselová, W. Wang, L. M. Wingen, E. M. Knipping, D. J. Tobias, D. Dabdub, and B. J. Finlayson-Pitts, J. Phys. Chem. A **108**, 11559 (2004).
[6]L. M. Wingen, A. C. Moskun, S. N. Johnson, J. L. Thomas, M. Roeselová, D. J. Tobias, M. T. Kleinman, and B. J. Finlayson-Pitts, Phys. Chem. Chem. Phys. **10**, 5668 (2008).
[7]P. Jungwirth and D. J. Tobias, Chem. Rev. **106**, 1259 (2006).
[8]P. Salvador, J. E. Curtis, D. J. Tobias, and P. Jungwirth, Phys. Chem. Chem. Phys. **5**, 3752 (2003).
[9]L. X. Dang, T.-M. Chang, M. Roeselova, B. C. Garrett, and D. J. Tobias, J. Chem. Phys. **124**, 66101 (2006).
[10]J. L. Thomas, M. Roeselová, L. X. Dang, and D. J. Tobias, J. Phys. Chem. A **111**, 3091 (2007).
[11]M. A. Brown, B. Winter, M. Faubel, and J. C. Hemminger, J. Am. Chem. Soc. **131**, 8354 (2009).
[12]D. E. Otten, P. B. Petersen, and R. J. Saykally, Chem. Phys. Lett. **449**, 261 (2007).
[13]Y. Levin, Phys. Rev. Lett. **102**, 147803 (2009).
[14]P. L. Geissler, Annu. Rev. Phys. Chem. **64**, 317 (2013).
[15]S. Vaikuntanathan, P. R. Shaffer, and P. L. Geissler, Faraday Discuss. **160**, 63 (2013).
[16]C. Caleman, J. S. Hub, P. J. van Maaren, and D. van der Spoel, Proc. Natl. Acad. Sci. U. S. A. **108**, 6838 (2011).
[17]D. E. Otten, R. Onorato, R. Michaels, J. Goodknight, and R. J. Saykally, Chem. Phys. Lett. **45**, 519–520 (2012).
[18]O. Shih, A. H. England, G. C. Dallinger, J. W. Smith, K. C. Duffey, R. C. Cohen, D. Prendergast, and R. J. Saykally, J. Chem. Phys. **139**, 035104 (2013).
[19]A. H. England, A. M. Duffin, C. P. Schwartz, J. S. Uejio, D. Prendergast, and R. J. Saykally, Chem. Phys. Lett. **514**, 187 (2011).
[20]R. K. Lam, A. H. England, A. T. Sheardy, O. Shih, J. W. Smith, A. M. Rizzuto, D. Prendergast, and R. J. Saykally, Chem. Phys. Lett. **614**, 282 (2014).
[21]J. W. Smith, R. K.-J. Lam, A. T. Sheardy, O. Shih, A. M. Rizzuto, O. Borodin, S. J. Harris, D. Prendergast, and R. J. Saykally, Phys. Chem. Chem. Phys. **16**, 23568 (2014).
[22]K. R. Wilson, B. S. Rude, T. Catalano, R. D. Schaller, J. G. Tobin, D. T. Co, and R. J. Saykally, J. Phys. Chem. B **105**, 3346 (2001).
[23]C. D. Cappa, J. D. Smith, K. R. Wilson, and R. J. Saykally, J. Phys.: Condens. Matter **20**, 205105 (2008).
[24]K. R. Wilson, B. S. Rude, J. Smith, C. Cappa, D. T. Co, R. D. Schaller, M. Larsson, T. Catalano, and R. J. Saykally, Rev. Sci. Instrum. **75**, 725 (2004).
[25]D. A. Case, J. T. Berryman, R. M. Betz, D. S. Cerutti, T. E. Cheatham III, T. A. Darden, R. E. Duke, T. J. Giese, H. Gohlke, A. W. Goetz, N. Homeyer, S. Izadi, P. Janowski, J. Kaus, A. Kovalenko, T. S. Lee, S. LeGrand, P. Li, T. Luchko, R. Luo, B. Madej, K. M. Merz, G. Monard, P. Needham, H. Nguyen, H. T. Nguyen, I. Omelyan, A. Onufriev, D. R. Roe, A. Roitberg, R. Salomon-Ferrer, C. L. Simmerling, W. Smith, J. Swails, R. C. Walker, J. Wang, R. M. Wolf, X. Wu, D. M. York, and P. A. Kollman, *AMBER 2015* (University of California, San Francisco, 2015).
[26]W. Humphrey, A. Dalke, and K. Schulten, J. Mol. Graphics **14**, 33 (1996).
[27]D. Prendergast and G. Galli, Phys. Rev. Lett. **96**, 215502 (2006).
[28]P. Giannozzi, S. Baroni, N. Bonini, M. Calandra, R. Car, C. Cavazzoni, D. Ceresoli, G. L. Chiarotti, M. Cococcioni, I. Dabo, A. Dal Corso, S. de. Gironcoli, S. Fabris, G. Fratesi, R. Gebauer, U. Gerstmann, C. Gougoussis, A. Kokalj, M. Lazzeri, L. Martin-Samos, N. Marzari, F. Mauri, R. Mazzarello, S. Paolini, A. Pasquarello, L. Paulatto, C. Sbraccia, S. Scandolo, G. Sclauzero, A. P. Seitsonen, A. Smogunov, P. Umari, and R. M. Wentzcovitch, J. Phys.: Condens. Matter **21**, 395502 (2009).
[29]J. P. Perdew, K. Burke, and M. Ernzerhof, Phys. Rev. Lett. **77**, 3865 (1996).
[30]J. A. Rodriguez, T. Jirsak, J. Dvorak, S. Sambasivan, and D. Fischer, J. Phys. Chem. B **104**, 319 (2000).
[31]B. M. Messer, C. D. Cappa, J. D. Smith, K. R. Wilson, M. K. Gilles, R. C. Cohen, and R. J. Saykally, J. Phys. Chem. B **109**, 5375 (2005).
[32]M. der M. Marcos-Arroyo, M. K. Khoshkbarchi, and J. H. Vera, J. Solution Chem. **25**, 983 (1996).
[33]B. R. Staples, J. Phys. Chem. Ref. Data **10**, 765 (1981).
[34]N. T. Skipper and G. W. Neilson, J. Phys.: Condens. Matter **1**, 4141 (1989).
[35]R. Mancinelli, A. Botti, F. Bruni, M. A. Ricci, and A. K. Soper, J. Phys. Chem. B **111**, 13570 (2007).
[36]G. W. Neilson, P. E. Mason, S. Ramos, and D. Sullivan, Philos. Trans. R. Soc., A **359**, 1575 (2001).
[37]J. A. White, E. Schwegler, G. Galli, and F. Gygi, J. Chem. Phys. **113**, 4668 (2000).
[38]M. Carrillo-Tripp, H. Saint-Martin, and I. Ortega-Blake, J. Chem. Phys. **118**, 7062 (2003).
[39]A. Bankura, V. Carnevale, and M. L. Klein, J. Chem. Phys. **138**, 014501 (2013).
[40]V. Vchirawongkwin, C. Kritayakornupong, A. Tongraar, and B. M. Rode, J. Phys. Chem. B **115**, 12527 (2011).
[41]S. Vchirawongkwin, C. Kritayakornupong, A. Tongraar, and V. Vchirawongkwin, Dalton Trans. **43**, 12164 (2014).
[42]H. Ohtaki and T. Radnai, Chem. Rev. **93**, 1157 (1993).
[43]P. A. Bergstroem, J. Lindgren, and O. Kristiansson, J. Phys. Chem. **95**, 8575 (1991).
[44]Y. Kameda, H. Arakawa, K. Hangai, and O. Uemura, Bull. Chem. Soc. Jpn. **65**, 2154 (1992).
[45]S. P. Dagnall, D. N. Hague, and A. D. C. Towl, J. Chem. Soc., Faraday Trans. **2**(78), 2161 (1982).
[46]V. Simeon, V. Butorac, V. Tomišić, and N. Kallay, Phys. Chem. Chem. Phys. **5**, 2015 (2003).
[47]X.-B. Wang, X. Yang, L.-S. Wang, and J. B. Nicholas, J. Chem. Phys. **116**, 561 (2002).
[48]R. Caminiti, G. Licheri, G. Piccaluga, and G. Pinna, J. Chem. Phys. **68**, 1967 (1978).
[49]A. M. Duffin, C. P. Schwartz, A. H. England, J. S. Uejio, D. Prendergast, and R. J. Saykally, J. Chem. Phys. **134**, 154503 (2011).
[50]W. L. Jorgensen, J. Chandrasekhar, J. D. Madura, R. W. Impey, and M. L. Klein, J. Chem. Phys. **79**, 926 (1983).
[51]J. J. P. Stewart, J. Comp. Chem. **10**, 209 (1989).